J. Chem. Thermodynamics 198 (2024) 107346

Contents lists available at ScienceDirect

The Journal of Chemical Thermodynamics

journal homepage: www.journals.elsevier.com/the-journal-of-chemical-thermodynamics

Phase transition study of bathophenanthroline and bathocuproine: A multitechnique approach

José M. Silva Ferraz [a], Lorenza Romagnoli [b], Bruno Brunetti [c], Andrea Ciccioli [b], Stefano Vecchio Ciprioti [d,*], Vera L.S. Freitas [a,*], Maria D.M.C. Ribeiro da Silva [a]

[a] CIQUP-IMS, Department of Chemistry and Biochemistry, Faculty of Sciences, University of Porto, Rua do Campo Alegre, P-4169-007 Porto, Portugal
[b] Dipartimento di Chimica, Sapienza University of Rome, P.le A. Moro 5, 00185 Rome, Italy
[c] Istituto per lo Studio dei Materiali Nanostrutturati, Consiglio Nazionale delle Ricerche, Dipartimento di Chimica, Sapienza Università di Roma, P.le A. Moro 5, 00185 Rome, Italy
[d] Dipartimento di Scienze di Base ed Applicate per l'Ingegneria (S.B.A.I.), Sapienza University of Rome, Via del Castro Laurenziano 7, Building RM017, 00161 Rome, Italy

ARTICLE INFO

Keywords:
Phenanthroline
Organic semiconductors
Thermal behaviour
Sublimation enthalpy
Phase transitions

ABSTRACT

The thermal behaviour of bathophenanthroline and bathocuproine has been studied using several techniques, namely, differential scanning calorimetry and thermogravimetry. To determine their respective enthalpies of sublimation, vapor pressure measurements were carried out using different methods, such as Knudsen effusion mass loss/mass spectrometry, isothermal thermogravimetry, and a quartz crystal microbalance technique. Furthermore, the enthalpies of sublimation were determined by measuring the heat change of the sublimation process using high-temperature Calvet microcalorimetry.

The results obtained in this work allowed the determination of the standard molar enthalpies of sublimation at 298.15 K, for bathophenanthroline and bathocuproine. The values obtained were (183.8 ± 2.2) kJ·mol^{-1} and (206.2 ± 2.8) kJ·mol^{-1}, respectively. Additionally, the standard molar enthalpies of fusion were determined to be (30.4 ± 0.4) kJ·mol^{-1} and (26.5 ± 1.6) kJ·mol^{-1} for bathophenanthroline and bathocuproine, respectively. The analysis of the results allows a deeper understanding of the phase transition behavior for these compounds from the condensed to the gaseous phases, elucidating molecular decomposition and the inherent intermolecular forces governing the species.

1. Introduction

Within the scope of our research on the thermodynamic characterization of nitrogen heterocyclic compounds [1–4], this study focuses on developing thermophysical experiments on two phenanthroline derivatives: bathophenanthroline (4,7-diphenyl-1,10-phenanthroline) and bathocuproine (2,9-dimethyl-4,7-diphenyl-1,10-phenanthroline) whose molecular structures are depicted in Fig. 1.

1,10-Phenanthroline is a relevant ligand in coordination chemistry due to its effective coordination with metals through multiple nitrogen donor atoms, presenting a distinctive blend of metal ion binding versatility and complex properties, thereby contributing significantly to coordination chemistry [5]. Metal complexes containing ligands based on 1,10-phenanthroline have been actively investigated for their redox, catalytic, photochemical, and photophysical properties, emerging as fundamental components in the development of efficient luminescent materials and, more recently, even photoswitchable molecular devices [6]. Compounds based on 1,10-phenanthroline are characterized as dipolar organic molecules, featuring potent electron-withdrawing nitrogen atoms and a low-lying lowest unoccupied molecular orbital (LUMO) [7,8]. Furthermore, the inherent *cis*-conformation of the 1,10-phenanthroline core offers several unique structural and chemical advantages. These attributes render phenanthroline derivatives effective as mediators for single-electron transfer processes, showcasing notable electron mobility and finding applications as reagents for energy transfer processes. In recent years, phenanthroline derivatives have demonstrated distinct charge mobility properties, excelling in both electron and hole transport, as well as in blocking their passage, thereby presenting potential for use as barrier or blocking materials in semiconductor devices or other applications requiring precise control of

* Corresponding authors.
E-mail addresses: stefano.vecchio@uniroma1.it (S.V. Ciprioti), vera.freitas@fc.up.pt (V.L.S. Freitas).

https://doi.org/10.1016/j.jct.2024.107346
Received 13 March 2024; Received in revised form 1 July 2024; Accepted 3 July 2024
Available online 6 July 2024

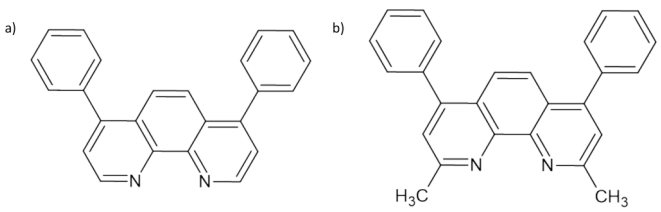

Fig. 1. Structural formulas of a) bathophenanthroline and b) bathocuproine.

charge flow [9–11]. Notably, bathophenanthroline and bathocuproine have been reported to exhibit high electron mobilities, comparable to other electron-transporting materials [12–14]. In fact, bathocuproine has been found to serve as effective hole-blocking layers for energy generation purposes [15].

The phase transition study of the two title compounds was developed using different techniques. Differential scanning calorimetry (DSC) and simultaneous thermal analysis (STA or DSC/TG) were employed to analyse their thermal behaviour.

Both direct and indirect approaches were employed to determine the enthalpy of sublimation for each compound. With Knudsen effusion mass loss (KEML) and Knudsen effusion mass spectrometry (KEMS), both classified as indirect methods, the vapor pressure as a function of temperature was obtained and subsequently utilized to calculate the enthalpy of sublimation. Conversely, direct methods such as high-temperature Calvet microcalorimetry (CM) directly measure the enthalpy of sublimation, which is proportionate to the heat involved in the sublimation process. Additionally, a quartz crystal microbalance was used to investigate the sublimation process under high-vacuum and non-equilibrium conditions.

Understanding the thermophysical characteristics of compounds associated with phenanthroline across different temperature ranges is crucial. This comprehension empowers researchers to optimize their properties and performance for a wide array of applications, while also ensuring safety and stability.

2. Experimental methodologies

2.1. Characterization and purity assessment of compounds

The samples of BP and BCP used in this work were acquired commercially with a minimum fractional purity of 0.997 (comprehensive information available in Table 1). The gas–liquid chromatography analysis performed on commercial samples of both compounds confirmed the high purity required to develop the thermophysical study, eliminating the need for a purification process.

The water content of both compounds, with results reported in Table 1, was determined through coulometric Karl Fischer titration. This analysis was conducted using a Metrohm 831 KF coulometer equipped with a diaphragm-free generator electrode, coupled with an oven (860 KF Thermoprep). The anolyte solution used was the Hydranal Coulomat AG-oven. The system performance was checked by Hydranal Water Standard KF-Oven 220 °C–230 °C, Cat. No 34748, Lot H038A. Sets of five experiments were conducted for each compound.

Details about other compounds used in this work are compiled in Table S1 of the Supplementary material.

The standard atomic weights of the elements used throughout this paper were those suggested by the IUPAC Commission in 2021 [16].

2.2. Thermal analysis

The Netzsch DSC 204 F1 Phoenix, a heat flux differential scanning calorimeter equipped with an intra-cooler unit, was used to determine the temperatures and enthalpies of fusion and to analyse the thermal behaviour of the title compounds. Subsequently, the acquired data underwent further analysis using the Netzsch Proteus Thermal Analysis 8.0.3 software. The DSC experiments aimed at determining the temperature and enthalpy of fusion of both compounds were conducted under a nitrogen flow rate of 40 $cm^3 \cdot min^{-1}$ as a purge and 20 $cm^3 \cdot min^{-1}$ as a protective gas, with heating rates of 2 $K \cdot min^{-1}$, using hermetically sealed aluminium crucibles. Additional experiments were also conducted employing different heating rates to explore the potential existence of multiple crystalline forms, providing insights into their relative stability.

Temperature and energy calibrations were performed at a heating rate of 2 $K \cdot min^{-1}$ using reference materials with a high degree of purity (samples description are provided in Table S1) and the respective standard molar enthalpy of fusion values, including indium (3284.0 $J \cdot mol^{-1}$ [17]), tin (7182.0 $J \cdot mol^{-1}$ [17]), bismuth (11097 $J \cdot mol^{-1}$ [17]), benzoic acid (17980 $J \cdot mol^{-1}$ [18]), naphthalene (18920 $J \cdot mol^{-1}$ [18]), cyclohexane (2652 $J \cdot mol^{-1}$ [19]), triphenylene (24744 $J \cdot mol^{-1}$ [18]), and biphenyl (18574 $J \cdot mol^{-1}$ [18]). In the case of adamantane, the standard molar enthalpy of the crystal-crystal phase transition (2997 $J \cdot mol^{-1}$ [17]) was used. For temperature and energy calibrations the parameters were, respectively $T_{fus\ (corr)} = 0.9961 \cdot T_{onset} + 0.08141$ and $K^{-1} = -0.0417 + 0.0279 \cdot T_{fus\ (corr)} + -6.62 \times 10^{-5}\ (T_{fus\ (corr)})^2 + 4.70 \times 10^{-8}\ (T_{fus\ (corr)})^3$.

Additionally, simultaneous thermogravimetric analysis (STA) analysis were performed using a Stanton-Redcroft 625 simultaneous TG/DSC apparatus connected to a 386 IBM-compatible personal computer. The system was calibrated using several high-purity standards, including tin and indium, tailored to the specific temperature range under investigation. Non-isothermal temperature experiments were carried out under a stream of synthetic air to observe the sample behaviour under more realistic conditions. The heating rate varied from among experiments, with precise specifications provided for each set. Open pan aluminium crucibles were used for the TG/DSC experiments, with each experiment employing 4 to 6 mg of the sample compound.

The DSC experiments were conducted under ambient pressure conditions, typically around 101.3 kPa (±2 kPa). Although the pressure was not controlled, this range represents the usual laboratory conditions during the experiments, with pressure variations (Δp) being approximately zero.

2.3. Calvet microcalorimetry

The calorimetric study was performed using a Calvet high temperature twin-microcalorimeter (Setaram HT1000D) employing the drop-calorimetric technique described by Skinner et al. [20]. Further details about the equipment and the methodology can be found in the literature

Table 1
Comprehensive information on the samples of the compounds studied.

Compound	Acronym	Cas Registry No.	Supplier	Massic fraction Purity	Water content (%)
Bathophenanthroline	BP	1662-01-7	Alfa Aesar	0.9998[a]	0.05[b]
Bathocuproine	BCP	4733-39-5	Acros Organics	0.9978[a]	0.07[b]

[a] The results, acquired via gas–liquid chromatography with a flame ionization detector, were obtained on a water-free basis. An Agilent 4890 apparatus equipped with an HP-5 column, which is cross-linked and composed of 5 % diphenyl and 95 % dimethylpolysiloxane (column dimensions: 15 m in length × 0.530 mm internal diameter × 1.5 μm film thickness) was used.
[b] Results obtained from coulometric Karl-Fischer titration.

[21].

Preliminary tests performed with the samples indicated that the programmed operating temperature of the Calvet microcalorimetry should be set at 511 K for BP and 541 K for BCP. The mass of the samples ranged from 3 to 4 mg. The thermal corrections for the different sensibilities of the two calorimetric cells and for the differences in the mass of the glass capillary tubes were determined in separate experiments. These corrections were minimized in each experiment by dropping capillary tubes of nearly equal mass, to within $\pm (1{\cdot}10^{-4})$ g, into each of the twin calorimetric cells.

The Calvet microcalorimeter was calibrated for each operating temperature using a recommended reference compound with a vapor pressure similar to that of the compounds under study, such as 1,3,5-triphenylbenzene.

2.4. Knudsen effusion method

The Knudsen effusion mass loss (KEML) experiments were carried out using a Ugine-Eyraud Model B60 Setaram thermobalance, as extensively described in a previous paper [22].

The equipment essentially consists of a furnace, a microbalance, and a vacuum system. The measuring cell is housed in a copper cylinder with a cap, designed to homogenize the temperature of the sample for precise temperature measurements. The copper cylinder is suspended to the arm of the microbalance with a standard measurement uncertainty $u(m) = 0.01$ mg. Temperature measurements were taken using a Pt100 Platinum Resistance Thermometer inserted into the copper cylinder, with the standard measurements uncertainty $u(T)$ being less than 0.2 K. Temperature control and mass loss measurements are made through a data logger (HP 34970A) controlled by a LabVIEW software, enabling continuous system monitoring and control.

During each KEML experiment, the temperature of the sample was adjusted to evaluate the mass loss rate at different constant temperatures, eventually converting it to vapour pressures via Eq. (1), where m is the sublimated mass of the compound during an effusion time period, t, at a specific temperature T of the experiment, and p corresponds to the vapour pressure. A_0 stands for the area of the effusion orifice, R is the gas constant ($R = 8.3144598$ J·K^{-1}·mol^{-1}) [23], M is the molar mass of the compound, and w_0 represents the Clausing probability factor.

$$p = \frac{1}{w_0}\cdot\frac{m}{A_0 t}\left(\frac{2\pi RT}{M}\right)^{1/2} \tag{1}$$

Afterward, a regression of $\ln p$ *vs* $1/T$ is performed to apply the Clausius Clapeyron relation and the following equations.

$$ln\left(\frac{p}{p^{\circ}}\right) = a - \left(\frac{b}{T}\right) \tag{2}$$

$$b = \frac{\Delta^{g}_{cr}H_m}{R} \tag{3}$$

$$\Delta^{g}_{cr}S_m(p,\langle T\rangle) = \frac{\Delta^{g}_{cr}H_m}{\langle T\rangle} \tag{4}$$

Knudsen effusion mass spectrometry experiments were also carried out as to observe the chemical composition of the effused gases [22,24]. A single focusing 90° magnetic sector mass spectrometer, originally developed by PATCO and equipped with a Knudsen molecular source, was employed for this purpose. The effusion cell used in this work is made of platinum and has an effusion orifice with 1 mm diameter. This Knudsen cell is inserted into an outer tantalum crucible. The effusion source is surrounded by a spiral-shaped tungsten heating element and tantalum shields positioned to achieve better thermal equilibrium. Temperature measurements are conducted using a W/Rh thermocouple inserted at the base of the tantalum crucible. Ionization of the vapours effusing from the Knudsen cell was accomplished through electron impact with an electron emission current generally regulated at 1.0 mA. The intensities were measured through a secondary electron multiplier.

The translation of the obtained signal to pressures is based on Eq. (5), where p_x is the partial pressure of a given species x, I^{+}_{nx} is the ion intensity of the isotope n of species x, K_{instr} is the instrumental constant of the ionization source, T is the temperature in K, σ_x is the ionization cross-section which measures the probability of ionization occurring when a molecule of the sample collides with an electron, γ_{nx} is the gain constant of the electron multiplier detector, and α_{nx} is the isotopic abundance.

$$p_x = \frac{K_{instr} I^{+}_{nx} T}{\sigma_x \gamma_{nx} \alpha_{nx}} \tag{5}$$

Note that, although it is not the main goal of this technique, it is also possible to determine some gas-phase ion energetic parameters such as the appearance energy, AE_0.

The measurements were carried out by filling a Knudsen cell with enough sample to cover its bottom and subsequently exposing it to a high vacuum. Once low background pressures are reached, the heating element is turned on. Temperature is generated by passing a high current (10–200 A) through the tungsten heating element. The temperature of the sample is monitored via a thermocouple in contact with the bottom of the Knudsen effusion cell, as mentioned before. When the T is considered stable, the measurement of ion beam intensity can be carried out. A shutter is placed in the way of the molecular source to distinguish the ions produced by a sample from the background gases with the same mass-to-charge ratio. It is also important to note that most measurements were done using an approximate 20 eV electron energy. The same process is done for an appropriate calibrant (in this case 1,3,5-triphenylbenzene) which will produce an instrumental constant.

The adjustment of the enthalpy and entropy values to the reference temperature was done in accordance with the method proposed by Chickos et al. [25,26], by considering the changes in heat capacity and vapour pressure between the average temperature and the reference temperature. This was accomplished through the following equations:

$$\Delta^{g}_{cr,l}H^{\circ}_m(298.15K) = \Delta^{g}_{cr,l}H^{\circ}_m(\langle T\rangle) + \left[C^{\circ}_p(cr,l) - C^{\circ}_p(g)\right][\langle T\rangle - 298.15] \tag{6}$$

$$\Delta^{g}_{cr,l}S^{\circ}_m(298.15K) = \Delta^{g}_{cr,l}S_m(\langle T\rangle, p\langle T\rangle) + \Delta^{g}_{cr}C^{\circ}_p\cdot\ln\left(\frac{298.15}{\langle T\rangle}\right) + R\cdot\ln\left(\frac{p^{\circ}}{p\langle T\rangle}\right) \tag{7}$$

2.5. Quartz crystal microgravimetry

Quartz Crystal Microgravimetry (QCMG) uses a quartz crystal microbalance (QCM) to determine the rate of mass deposition on a quartz crystal. This rate is proportional to the rate of mass-loss of a sample at a pre-defined temperature. By acquiring a sufficient number of data points over a large enough T range, it becomes feasible to plot $\ln Q$ *vs* $1/T$ to determine the heat of transition from a condensed phase to the gaseous phase using an adapted Clausius-Clapeyron relation.

Quartz crystal-based microbalances have been used in microgravimetric techniques to determine the deposition of very small masses [27–29]. This can be done as the increase in thickness of the "load" on the quartz crystal results in a decrease in its resonant frequency. The first developments of this technique appeared in 1959 when Sauerbrey introduced this new mass measuring method [30]. It has been shown that QCMG is highly sensitive to small changes in mass of solid samples [31].

The working principles of this apparatus are based in open cell conditions (non-equilibrium) rather than Knudsen conditions (effusion through an orifice, under equilibrium). Nevertheless, this technique uses an adapted Clausius-Clapeyron relation [32,33]. The Sauerbrey relation, $df = -Cf^2 dm S_C^{-1}$ [20], is used, considering that the change in frequency

over time is directly proportional to the change in mass over time, $\frac{df}{dt} \approx \frac{dm}{dt}$. Consequently, it is possible to derive Eq. (8), where $\frac{df}{dt}\sqrt{T} = Q$. It is important to note that this working equation only accounts for the process of phase change and not any other process that might occur, such as condensation of the evolved gas. This, of course, introduces an error that must be taken into consideration when conducting measurements with this technique.

$$\ln\left(\frac{df}{dt}\sqrt{T}\right) = -\frac{\Delta^{g}_{cr,l}H^{\circ}_{m}}{RT} + A \tag{8}$$

The equipment used in this setup comprises both commercial and specially crafted parts. Originally designed to study ionic liquids at lower temperatures than other devices found in literature, its designed is based on the work developed by Verevkin et al [33].

The measurement procedure follows a step-temperature approach, where a pre-defined change in frequency is observed at a certain temperature. The duration of the change in frequency is recorded, from which the $\frac{df}{dt}$ value is obtained. This value will be used in the ln Q vs $1/T$ plot. Frequency measurements are done with a shutter that either exposes or blocks the QCM to the vapour of the sample.

3. Results and discussion

3.1. Temperatures and enthalpies of fusion

The experiments to determine the enthalpy and temperature of fusion of BP were conducted in the temperature range of [298.15–513.15] K at heating rate of 2 K·min^{-1}. From four different experiments using fresh samples, a value of (492.46 ± 0.78) K was obtained for the temperature of fusion, along with a value of (41.0 ± 0.4) kJ·mol^{-1} for the standard molar enthalpy of fusion. The results are presented in Table 2, including the final mean value adjusted to the reference temperature of 298.15 K.

In Fig. 2, a close-up view of the fusion peak of BP is presented, obtained at a heating rate of 10 K·mol^{-1}, to highlight or clarify specific thermal effects. As mentioned earlier, this is a single sharp endothermic peak, indicating the presence of a single crystalline form that undergoes rapid melting in a single step.

The experiments to determine the enthalpy and temperature of fusion of BCP were conducted in the temperature range of [298.15–573.15] K at a heating rate of 2 K·min^{-1}. From four different experiments using fresh samples, a value of (554.83 ± 0.74) K was obtained for the temperature of fusion, along with a value of (40.5 ± 1.6) kJ·mol^{-1} for the standard molar enthalpy of fusion at the average temperature of fusion. These values, along with the adjusted value to the reference temperature, are presented in the Table 3 with a 0.95 level of confidence.

Table 2
Fusion enthalpy values at the fusion temperature obtained for bathophenanthroline (BP) by differential scanning calorimetry.

Experiments	Bathophenanthroline	
	T_{fusion} (K)	$\Delta^{l}_{cr}H^{\circ}_{m}$ <T_{fusion}> (kJ·mol^{-1})
1	492.27	41.1
2	492.26	41.1
3	492.55	40.9
4	492.77	40.8
Average Values	⟨492.46 ± 0.78⟩ [a]	⟨41.0 ± 0.4⟩ [a]
$\Delta^{l}_{cr}H^{\circ}_{m}$(298.15K)(kJ·mol^{-1})	30.4 ± 0.4[a]	

[a] The uncertainty quoted corresponds to the expanded uncertainty obtained from the combined standard uncertainty (which include the calibration) and the coverage factor k = 3.182 for a 0.95 level of confidence.

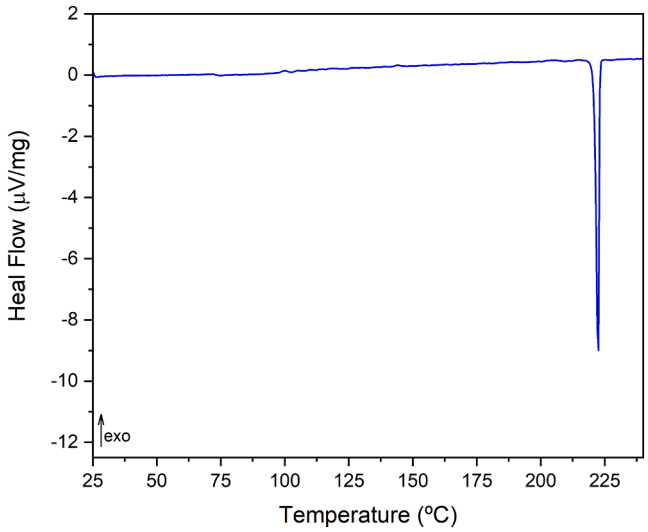

Fig. 2. Thermogram of a 10 K·min^{-1} scan of the original bathophenanthroline (BP) sample. Analysis conducted with a hermetically sealed alluminium crucible under a constant nitrogen flow.

Table 3
Fusion enthalpy values at the fusion temperature obtained for bathocuproine (BCP) by differential scanning calorimetry.

Experiments	Bathocuproine	
	T_{fusion} (K)	$\Delta^{l}_{cr}H^{\circ}_{m}$/ <$T_{fusion}$> (kJ·mol^{-1})
1	554.52	40.46
2	555.01	39.84
3	555.01	40.60
4	554.79	41.02
Average Values	⟨554.83 ± 0.74⟩ [a]	⟨40.5 ± 1.6⟩ [a]
$\Delta^{l}_{cr}H^{\circ}_{m}$ (298.15K)(kJ·mol^{-1})	26.5 ± 1.6[a]	

[a] The uncertainty quoted corresponds to the expanded uncertainty obtained from the combined standard uncertainty (which include the calibration) and the coverage factor k = 3.182 for a 0.95 level of confidence.

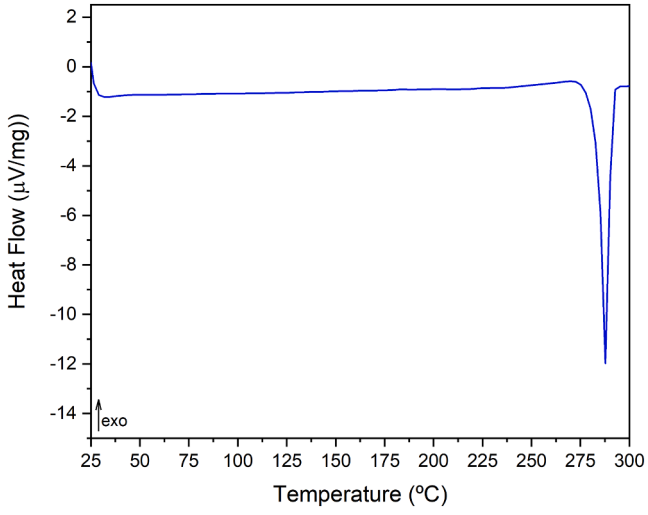

Fig. 3. DSC curve of a 10 K·min^{-1} scan of the original bathocuproine (BCP) sample. Analysis conducted with a hermetically sealed aluminium crucible under a constant nitrogen flow.

In Fig. 3, the fusion peak for BCP is depicted. As mentioned previously, it is a single yet elongated endothermic peak, suggesting the presence of a single crystalline form. However, the elongated nature may indicate the occurrence of another simultaneous process. This process appears to be decomposition based on data collected from the DSC/TG experiments.

3.2. Thermal behaviour

A DSC scan at 10 K·min^{-1} of a BP sample between [513.15–213.15] K and subsequently between [213.15–513.15] K indicated the presence of several thermophysical phenomena deserving further study. In the order of occurrence, these were: (a) a change in the baseline of the DSC signal, (b) an exothermic peak, (c) an endothermic peak followed by (d) an exothermic peak, and finally (e) an endothermic peak. This is further detailed in Fig. 4. Event (a) has been identified as an artifact of the cooling system and has no thermophysical significance. The exothermic nature of event (b) suggests that the sample may be undergoing transformation into a solid metastable state, as the amount of energy involved is very small. Complementary FTIR analysis of the sample between points (b) and (c) reveals a similar chemical bond but with the distinct presence of an N-H bond, which appears to be the reason for the stability of this intermediary. The spectra of the original sample versus the metastable sample are shown in Fig. 5. The endothermic nature of event (c) suggests a transition from an organized state to a less organized one, most likely an isotropic liquid. This transition provides enough mobility to the sample to crystallize into a thermodynamically stable state fully at (d). Event (e) is attributed to fusion.

The behaviour described above is reproducible over several cycles with no significant variation of temperature or heat of fusion. Further FTIR analysis of the recrystallized sample shows that there is no chemical difference between the samples.

A 10 K·min^{-1} heating scan from room temperature (RT) to 873.15 K was performed using the STA apparatus described in the experimental section and the DSC/TG curves obtained for BP are presented in Fig. 6.

Before fusion, stable heat flow and mass signals indicate that no detectable change is observed in the sample, i.e., no significant decomposition and no significant sublimation occur. After fusion, a constant decrease in the heat flow of the sample is observed. The shape of the DSC signal may be indicative of vaporization of the sample, i.e., an endothermic loss of mass. Although decomposition cannot be completely ruled out, the signal indicates that none occurs as no exothermic events are observed. It is also important to note a 90 % decrease in the mass sample. The 90 % decrease in mass ends around $T \approx$ 700.15 K, after which a substantial exothermic heat flow change is observed. This change indicates the thermal decomposition of the remaining sample. At $T \approx$ 823.15 K, the experiments reach their conclusion with a complete mass loss.

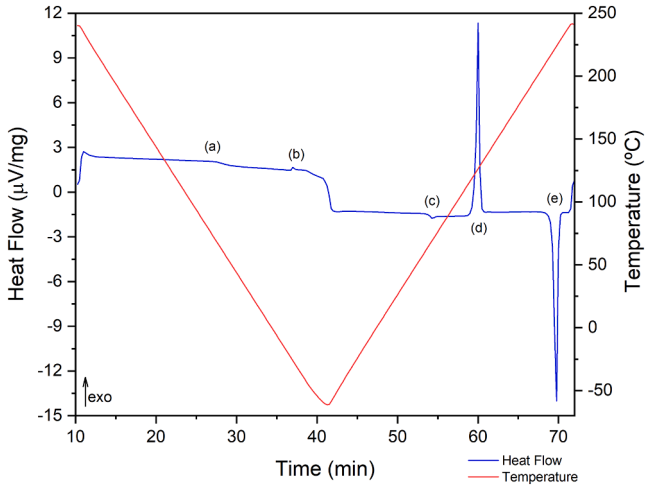

Fig. 4. DSC curve of the thermal behaviour analysis of bathophenanthroline (BP). Hermetically sealed Al crucible under N_2 flow.

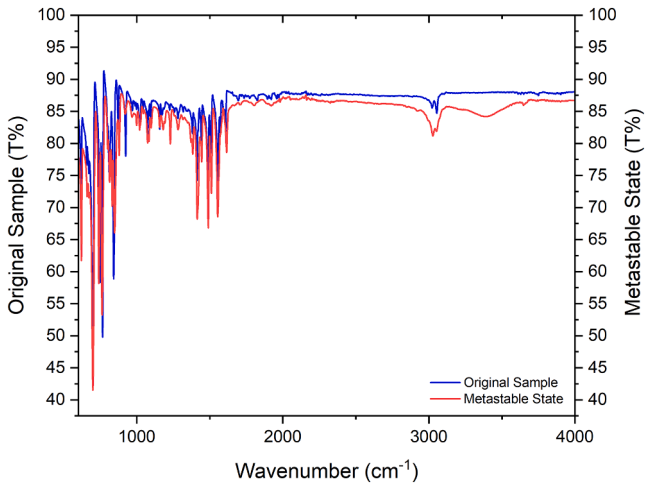

Fig. 5. Bathophenanthroline (BP) FTIR spectra. Original sample versus metastable sample.

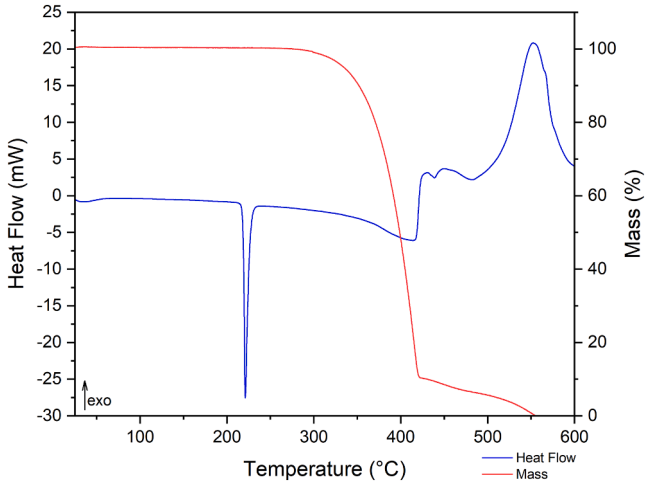

Fig. 6. DSC and TG curves of bathophenanthroline (BP) under open Al crucible and synthetic air conditions. [RT – 873.15] K range.

Similar experiments were conducted on BCP samples, and the results are now presented. A scan with a heating rate of 10 K·min^{-1} was performed between [573.15–213.15] K and subsequently between [213.15–573.15] K. Unlike BP, BCP does not exhibit any unusual thermophysical events. Only fusion and crystallization are observed.

A heating scan at a rate of 10 K·min^{-1} from RT to 873.15 K, was performed using the STA apparatus described in the experimental section, and the DSC/TG curves obtained for BCP are presented in Fig. 7.

After fusion, a constant increase in the heat flow of the sample is observed, accompanied by an approximate mass loss of 26 %. The heat flow change is characteristic of the continuous thermal decomposition of the sample. The mass change appears to be approximately equivalent to the loss of a phenyl group and a methyl group. The decrease in the signal is constant until it reaches a minimum. This is indicative of the formation of an intermediate. Possible molecular structures are shown in Fig. 8. Further TG-MS or TG-FTIR experiments would shed light on this question.

After 743 K, several decomposition steps are observed: first two small steps followed by a massive exothermic signal. The proximity of these

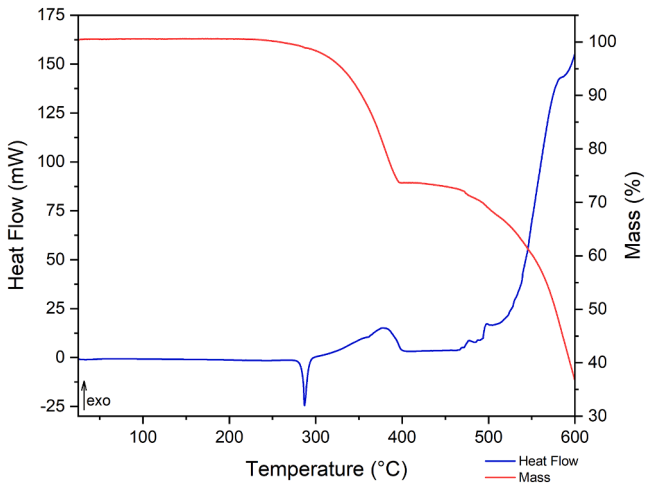

Fig. 7. DSC and TG curves of bathocuproine (BCP) under open crucible and synthetic air conditions. [RT – 873.15] K range.

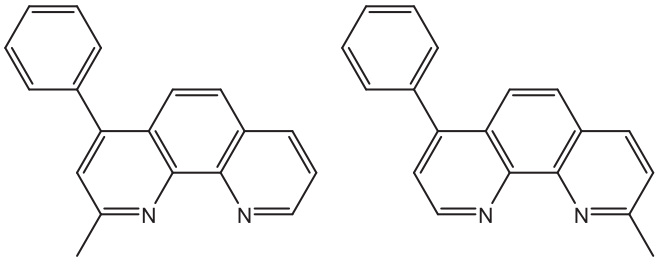

Fig. 8. Possible molecular structure of the intermediate molecules formed after thermal decomposition.

events makes their distinction difficult. The experiment ends with an exothermic signal that cannot be fully accounted for as the device has reached its maximum working temperature. These experiments were repeated several times, and the observed behaviour is reproducible.

3.3. Vapour pressures and enthalpies of sublimation

As mentioned in the previous section, the compounds under study underwent sublimation analysis using four different techniques: Calvet microcalorimetry (CM), quartz crystal microgravimetry (QCM) and two Knudsen effusion methods – mass loss (KEML) and mass spectrometry (KEMS).

With the vacuum drop-microcalorimetry technique, the obtained values for $\Delta^{g}_{cr}H^{\circ}_{m}$, at $T = 298.15$ K for BP and BCP were (183.7 ± 4.2) kJ·mol^{-1} and (206.9 ± 3.2) kJ·mol^{-1}, respectively. Detailed results of their respective experiments can be found in Tables 4 and 5. Appropriate temperature calibrations and testing experiments were performed using reference compound (1,3,5-triphenylbenzene) and a test sample (9-acridanone [34]). These results are presented in Supplementary information (Tables S2 to S5). In the case of the test sample, the results obtained agree, considering the given uncertainty, with the data provided in the literature.

Both phenanthroline derivatives underwent vapor pressure experiments using the Knudsen Effusion Method. The results of the vapor pressure at the different temperatures obtained from the Knudsen effusion experiments for the two compounds are listed in Tables 6 and 7.

The plots of ln(p/Pa) against 1/T, for the overall results obtained for BP and BCP are shown in Figs. S1 and S2, respectively, given in Supplementary information, with their corresponding parameters registered in Table 8. The values of the standard molar enthalpy, entropy, and Gibbs energy of sublimation, at $T = 298.15$ K, are reported in Table 9, with the uncertainties falling within the 95 % confidence interval.

Note that the uncertainty associated with the sublimation properties of BCP is relatively large due to a lower number of data points that could be collected and the larger spread of values around the fitting line.

As previously mentioned, alongside KEML experiments, KEMS measurements were performed on the two compounds under study. The main objective of these experiments was to assess the composition of the vapor phase and particularly ascertain the absence of volatile decomposition products. Notably, the only significant signal observed at $m/z =$ 332 (BP) and $m/z = 360$ (BCP), corresponding to the most abundant isotopes of the molecular ions, suggests the absence of detectable decomposition besides sublimation. This observation is further

Table 4
Experimental results of the sublimation study of bathophenanthroline (BP) obtained with the vacuum drop-microcalorimetry technique.[a]

	1	2	3	4	5	6
T/K[b]	511.28	511.18	511.42	511.18	511.18	511.34
m_{sct}/mg	24.6285	22.9686	22.7055	22.5858	22.4085	23.4417
m_{rct}/mg	24.5424	22.9937	22.6849	22.6550	22.4719	23.4313
m_{cpd}/mg	3.177	2.948	2.792	2.826	2.431	3.171
ΔH(blank)/mJ	31.215	52.423	46.514	60.047	59.714	45.834
ΔH(total)/J	2.232	2.057	1.940	1.981	1.652	2.184
ΔH(corr)/J	2.263	2.109	1.987	2.041	1.711	2.230
$\Delta^{g,T}_{cr,298.15}H^{\circ}_{m}$/kJ·mol^{-1}	258.7	259.8	258.4	262.3	255.6	255.4
$\Delta^{T}_{298.15}H^{\circ}_{m}$/kJ·mol^{-1}	74.6	74.6	74.7	74.6	74.6	74.7
$\Delta^{g}_{cr}H^{\circ}_{m}$(298.15K)/kJ·mol^{-1}	184.1	185.2	183.7	187.7	181.0	180.8

$< \Delta^{g}_{cr}H^{\circ}_{m}(298.15K) > = 183.7 \pm 4.2$ kJ·mol^{-1} [c]

[a] The symbols presented have the following meaning: T, temperature of the hot reaction vessel; m(sct) mass of the sample capillary tube; m(rct) mass of the reference capillary tube; m(cpd), mass of the compound corrected for buoyancy; ΔH(blank), blank heat capacity corrections for the glass capillary tubes; ΔH(total), total enthalpy calculated from the area of the enthalpic peak obtained in the experiment; ΔH(corr), enthalpy change corrected taking into account the blank experiments, calculated from $\Delta H(\text{corr}) = \Delta H(\text{total}) + \Delta H(\text{blank})$; $\Delta^{g,T}_{cr,\,298.15}H^{\circ}_{m}$ (exp), enthalpy of sublimation from 298.15 K to temperature of the hot reaction vessel calculated from $\Delta^{g,T}_{cr,\,298.15}H^{\circ}_{m} = [k_{cal}\cdot\Delta H(\text{corr})\cdot M]/m(\text{cpd})$, where k_{cal} is the calibration constant of the calorimeter for the experimental conditions and M the molar mass of the compound; $\Delta^{T}_{298.15}H^{\circ}_{m}$(g), enthalpy change in the gas-phase phase from 298.15 K to the temperature of the hot reaction vessel; $\Delta^{g}_{cr}H^{\circ}_{m}$(298.15 K), enthalpy of sublimation at 298.15 K of the compound calculated from $\Delta^{g}_{cr}H^{\circ}_{m}(298.15\text{ K}) = \Delta^{g,T}_{cr,\,298.15}H^{\circ}_{m} - \Delta^{T}_{298.15}H^{\circ}_{m}$(g).

[b] The standard uncertainty of the temperature measurements is $u(T/\text{K}) = 0.01$.

[c] The quoted uncertainty corresponds to the expanded uncertainty determined from the combined standard uncertainty (which include the contribution of calibration with 1,3,5-triphenylbenzene) and the coverage factor $k = 2.13$ (for an effective degrees of freedom of 15, calculated from Welch-Satterthwaite formula, and a 0.95 level of confidence) [35].

Table 5
Experimental results of the sublimation study of bathocuproine (BCP) obtained with the vacuum drop-microcalorimetry technique.[a]

	1	2	3	4	5	6	7
T/K[b]	541.08	541.12	541.11	541.13	541.02	541.02	541.12
m_{sct}/mg	23.9413	22.3607	22.5444	21.5358	21.7837	24.2976	24.9127
m_{rct}/mg	23.9004	22.3296	22.5668	21.5715	21.7284	24.1926	24.9887
m_{cpd}/mg	4.148	4.088	3.475	3.092	3.617	3.777	3.971
ΔH(blank)/mJ	42.225	49.191	57.567	63.155	47.027	30.271	58.654
ΔH(total)/J	3.120	3.044	2.568	2.262	2.688	2.866	2.994
ΔH(corr)/J	3.162	3.093	2.626	2.325	2.735	2.897	3.053
$\Delta^{g,T}_{cr,298.15}H^{\circ}_m$/kJ·mol^{-1}	295.9	293.6	293.2	291.9	293.4	297.6	298.4
$\Delta^{T}_{298.15}H^{\circ}_m$/kJ·mol^{-1}	87.9	87.9	87.9	87.9	87.9	87.9	87.9
$\Delta^{g}_{cr}H^{\circ}_m(298.15K)$/kJ·mol^{-1}	208.0	205.7	205.3	203.9	205.5	209.8	210.5

$< \Delta^{g}_{cr}H^{\circ}_m(298.15K) > = 206.9 \pm 3.2$ kJ·mol^{-1} [c]

[a] The symbols presented in this table have the same meaning as the symbols in the table above.
[b] The standard uncertainty of the temperature measurements is $u(T/K) = 0.01$.
[c] The quoted uncertainty corresponds to the expanded uncertainty determined from the combined standard uncertainty (which include the contribution of calibration with 1,3,5-triphenylbenzene) and the coverage factor $k = 2.13$ (for an effective degrees of freedom of 15, calculated from Welch-Satterthwaite formula, and a 0.95 level of confidence) [32].

Table 6
Saturated vapor pressures of crystalline bathophenanthroline (BP) in the temperature range of 427.2–468.0 K obtained from Knudsen effusion mass loss method.

T/K[a]	p/Pa[b]	ln (p/Pa)
427.2	0.010	−4.58
430.9	0.012	−4.40
431.0	0.012	−4.41
431.3	0.013	−4.31
435.5	0.025	−3.71
435.6	0.025	−3.69
437.5	0.027	−3.60
438.7	0.037	−3.31
439.0	0.033	−3.41
443.6	0.055	−2.91
443.8	0.062	−2.79
444.5	0.053	−2.94
447.5	0.088	−2.43
448.3	0.081	−2.51
450.1	0.127	−2.06
450.5	0.118	−2.14
451.5	0.128	−2.06
455.0	0.173	−1.75
455.2	0.209	−1.57
456.2	0.212	−1.55
458.7	0.266	−1.32
459.5	0.266	−1.32
462.3	0.438	−0.826
463.5	0.390	−0.942
465.6	0.540	−0.616
466.5	0.480	−0.734
468.0	0.713	−0.338

[a] The standard uncertainty in the measured temperature is $\pm(2{\cdot}10^{-1})$ K.
[b] The standard uncertainty is $\pm(0.1p)$ Pa.

supported by the XRD patterns recorded before and after the KEMS experiments, which showed no evident difference.

It is worth noting that the superior sensitivity of KEMS compared to KEML apparatuses facilitated exploration of a lower temperature range. Despite the approximate estimation of the ionization cross sections (see Supplementary Information), a satisfactory agreement is found between KEML- and KEMS-derived vapor pressures for both compounds. In addition, an attempt was made to estimate the sublimation enthalpy from KEMS vapor pressures. However, the limited number of data points may compromise the reliability of the slope.

The values of the standard molar enthalpy, entropy, and Gibbs energy of sublimation, at $T = 298.15$ K, are reported in Table 10, along with the appearance potential determined experimentally. Details on

Table 7
Saturated vapor pressures of crystalline bathocuproine (BCP) in the temperature range of 456.9–476.5 K obtained from Knudsen effusion mass loss method.

T/K[a]	p/Pa[b]	ln (p/Pa)
456.9	0.059	−2.83
461.2	0.096	−2.34
464.8	0.128	−2.06
468.2	0.193	−1.65
469.0	0.233	−1.46
471.9	0.282	−1.27
473.0	0.333	−1.10
475.7	0.428	−0.85
476.5	0.516	−0.66

[a] The standard uncertainty in the measured temperature is $\pm(2{\cdot}10^{-1})$ K.
[b] The standard uncertainty is $\pm(0.1p)$ Pa.

Table 8
Parameters of the Clausius-Clapeyron equation (a and b) for the two phenanthroline derivatives studied, along with calculated values for the enthalpy and entropy at the mean temperature of the experiments using the KEML method.

a	b	R^2	p (<T>) Pa	$\Delta^{g}_{cr}H^{\circ}_m(\langle T\rangle)$ kJ·mol^{-1}	$\Delta^{g}_{cr}S_m(\langle T\rangle, p\langle T\rangle)$ J·K^{-1}·mol^{-1}
Bathophenanthroline $\langle T\rangle = 448$ K					
44.63 ± 0.75[a]	−21076 ± 334[a]	0.9935	0.074	175.2 ± 2.8[c]	391.2 ± 6.2[c]
Bathocuproine $\langle T\rangle = 467$ K					
47.87 ± 1.49[b]	−23161 ± 696[b]	0.9937	0.154	192.6 ± 5.8[c]	412.6 ± 12.4[c]

[a] The standard uncertainty were obtained by multiplying the standard error of the fitting parameters by k = 2.06, that corresponds to the t-distribution value for 0.95 level of confidence and 25 degrees of freedom.
[b] The standard uncertainty were obtained by multiplying the standard error of the fitting parameters by k = 2.36, that corresponds to the t-distribution value for 0.95 level of confidence and 7 degrees of freedom.
[c] The uncertainties quoted correspond to the expanded uncertainties with a confidence level of 0.95.

the vapor pressures, Clausius Clapeyron equation parameters and calibration data are reported on Supplementary information (Tables S6 to S10). Their uncertainties are within the 0.95 level of confidence.

While the sublimation enthalpy obtained from KEMS data for BP (178.2 ± 1.8 kJ·mol^{-1} at 298.15 K) is still in acceptable agreement with the KEML and CM results, the value for BCP (186.8 ± 7.2 kJ·mol^{-1}) is

Table 9
Standard molar enthalpy, entropy, and Gibbs energy of sublimation obtained with KEML, at $T = 298.15$ K.[a]

Compound	$\Delta^{g}_{cr}H^{o}_{m}$/kJ·mol^{-1}	$\Delta^{g}_{cr}S^{o}_{m}$/J·K^{-1}·mol^{-1}	$\Delta^{g}_{cr}G^{o}_{m}$/kJ·mol^{-1}	p/Pa
BP	183.8 ± 2.8	255.0 ± 6.2	107.8 ± 3.1	3.49 × 10^{-10}
BCP	204.1 ± 5.8	248.6 ± 12.3	129.9 ± 7.5	1.07 × 10^{-11}

[a] The uncertainties quoted correspond to the expanded uncertainties with a confidence level of 0.95.

significantly lower, even considering the rather large associated error, than those derived from the other techniques. While it is challenging to provide a satisfactory explanation for the observed discrepancy, a possible underestimate of temperature might be considered to account for it.

BP and BCP were also studied using the quartz crystal microgravimetric (QCM) technique described earlier. The values for df/dt, T, $1/T$, and ln Q can be found in the Supplementary information (Tables S11 to S16). From these values, it is possible to calculate the enthalpy of sublimation at mean temperature, $\Delta^{g}_{cr}H^{*}_{m}(<T>)$, and subsequently, the enthalpy of sublimation at the reference temperature of 298.15 K, $\Delta^{g}_{cr}H^{*}_{m}$, with values in Table 11.

To correct the slope, a correction constant was obtained by measuring the df/dt values of 1,3,5-triphenylbenzene and calculating the sublimation enthalpy, comparing it with the value from literature (Tables S17, S18 and S19). The instrumental constant obtained can be used to correct the ln Q vs $1/T$ slope of the sample. These experiments were performed with a similar temperature program. The results obtained with the QCM method are presented in Table 11.

Regarding BP and BCP, the experimentally obtained results for the standard molar enthalpy of sublimation at the reference temperature of 298.15 K are registered in Table 12.

The standard molar enthalpy of sublimation at the reference temperature for BP, as determined by the KEML method, shows excellent agreement with the value obtained through the CM method. Therefore, it is advisable to use the mean of these two values. As for BCP, the value obtained with the KEML method also corresponds well with that obtained by the CM method. It is important to note that the software error mentioned earlier could be the primary reason for the difference observed, although decomposition cannot be ruled out entirely. Hence, it is recommended to use the mean of the two values, taking into account their standard deviations.

From the comparison of the values of the standard molar enthalpies of sublimation determined in this work by various techniques, it is evident that there is good agreement among them. Notably, the smallest difference is observed between KEML and CM, with a variance of no more than 2 kJ·mol^{-1}. Therefore, it is recommended to use the mean value, considering their standard deviations, for the enthalpy of sublimation: $\Delta^{g}_{cr}H^{*}_{m} = (183.8 \pm 2.2)$ kJ·mol^{-1} for BP and $\Delta^{g}_{cr}H^{*}_{m} = (206.2 \pm 2.8)$ kJ·mol^{-1} for BCP.

4. Conclusions

An extensive study on the three main phases of BP and BCP was conducted and presented in this paper, providing phase change information and thermophysical parameters for two compounds.

The standard molar enthalpies of sublimation at 298.15 K serve as a direct indication of the strong intermolecular forces present in the crystalline phase of both samples. In the case of BCP, a higher enthalpy of sublimation value is observed. This is most likely due to the insertion of the two methyl groups, which likely contribute to the stabilization of the electronic structure, particularly due to their proximity to the nitrogen atoms in the 1 and 10 positions of the structure.

It is noteworthy that BP exhibits several successive thermophysical phenomena in its condensed phases. The occurrence of a metastable phase followed by subsequent cold crystallization is relatively uncommon among small organic molecules, yet it appears to be a characteristic feature of the thermal behaviour of BP.

The TG/DSC analysis of the liquid phase indicates that BP remains stable until approximately 700 K, the temperature at which vaporization ends and thermal decomposition starts. This is also confirmed by the large standard molar enthalpy of vaporization at 298.15 K, obtained by calculating it using the enthalpies of fusion and sublimation. However, from DSC and TG experiments, it is evident that BCP starts to decompose after fusion, and the formation of an intermediary compound is hypothesized.

All of the values for the standard molar enthalpies of phase transition at 298.15 K are presented in Table 13.

CRediT authorship contribution statement

José M. Silva Ferraz: Writing – original draft, Investigation, Formal analysis. **Lorenza Romagnoli:** Investigation. **Bruno Brunetti:**

Table 11
Standard molar enthalpy at the mean temperature and at the temperature of 298.15 K before and after correction for bathophenanthroline (BP) obtained with the QCM method.

Compound	$\Delta^{g}_{cr}H^{*}_{m}(T = 298.15\text{K})$	$\Delta^{g}_{cr}H^{*}_{m}(T = 298.15\text{K})_{corr}$
	kJ·mol^{-1}	kJ·mol^{-1}
BP	161.6 ± 2.7	182.4 ± 4.5 [a,b]
BCP	177.6 ± 2.1	198.3 ± 4.4 [a,b]

[a] The uncertainties quoted correspond to the expanded uncertainties with a confidence level of 0.95.
[b] Obtained with an instrumental constant from 1,3,5-triphenylbenzene that is reported in table S19.

Table 12
Collection of the standard molar enthalpy of sublimation at the reference temperature of 298.15 K obtained for bathophenanthroline (BP) and bathocuproine (BCP).[a]

Techniques	$\Delta^{g}_{cr}H^{\hat{A}^{\circ}}_{m}$/kJ·mol^{-1}	
	BP	BCP
KEML	183.8 ± 2.8	204.1 ± 5.8
KEMS	178.2 ± 1.8	186.8 ± 7.2
QCM	182.4 ± 4.5	198.3 ± 4.4
CM	183.7 ± 4.2	206.9 ± 3.2
Recommended Value from KEML & CM	183.8 ± 2.2	206.2 ± 2.8

[a] The uncertainties quoted correspond to the expanded uncertainties with a confidence level of 0.95.

Table 10
Standard molar enthalpy, entropy, and Gibbs energy of sublimation obtained with KEMS, at $T = 298.15$ K.[a]

Compound	$\Delta^{g}_{cr}H^{*}_{m}$/kJ·mol^{-1}kJ·mol^{-1}	$\Delta^{g}_{cr}S^{*}_{m}$/J·K^{-1}·mol^{-1}·	$\Delta^{g}_{cr}G^{*}_{m}$/kJ·mol^{-1}·	p/Pa	AE_0/eV
BP	178.2 ± 1.8	318.3 ± 4.5	83.3 ± 1.5	7.11 × 10^{-11}	8.1 ± 0.2
BCP	186.8 ± 7.2	343.1 ± 18.2	84.5 ± 5.6	6.04 × 10^{-12}	8.9 ± 0.2

[a] The uncertainties quoted correspond to the expanded uncertainties with a confidence level of 0.95.

Table 13
Standard molar enthalpies of phase transition at the reference temperature of 298.15 K for bathophenanthroline (BP) and bathocuproine (BCP).

$\Delta^{l}_{cr}H^{\circ}_{m}$/kJ·mol^{-1}	$\Delta^{g}_{l}H^{\circ}_{m}$/kJ·mol^{-1}	$\Delta^{g}_{cr}H^{\circ}_{m}$/kJ·mol^{-1}
BP		
30.4 ± 0.4	153.4 ± 1.9	183.8 ± 2.2
BCP		
26.5 ± 1.6	179.7 ± 4.1	206.2 ± 2.8

Investigation. **Andrea Ciccioli:** Writing – review & editing, Supervision, Investigation. **Stefano Vecchio Ciprioti:** Writing – review & editing, Supervision, Investigation. **Vera L.S. Freitas:** Writing – review & editing, Supervision, Investigation, Formal analysis, Conceptualization. **Maria D.M.C. Ribeiro da Silva:** Writing – review & editing, Supervision.

Declaration of competing interest

The authors declare the following financial interests/personal relationships which may be considered as potential competing interests: Vera L. S. Freitas reports financial support was provided by Portuguese Foundation for Science and Technology. Jose M. Silva Ferraz reports financial support was provided by Erasmus Plus. We would like to declare that two of the authors, Vera L. S. Freitas and Stefano Vecchio Ciprioti serve as guest editors for the special issue selected. If there are other authors, they declare that they have no known competing financial interests or personal relationships that could have appeared to influence the work reported in this paper.

Data availability

Data will be made available on request.

Acknowledgements

The authors acknowledge the Fundação para a Ciência e Tecnologia (FCT) for financial support through projects UIDB/QUI/00081/2020 (https://doi.org/10.54499/UIDB/00081/2020) and IMS-(LA/P/0056/2020). VLSF thanks FCT for funding under reference DL 57/2016/CP1454/CT0019 (https://doi.org/10.54499/DL57/2016/CP1454/CT0019). JMSF thanks the European Union for funding the Erasmus+ project, under which some of the work was developed.

Appendix A. Supplementary data

Supplementary data to this article can be found online at https://doi.org/10.1016/j.jct.2024.107346.

References

[1] M.G. Bonicelli, A. Catalani, G. Mariano, S. Vecchio, Heat capacities and molar enthalpies and entropies of fusion for anhydrous 1,10-phenanthroline and 2,9-dimethyl-1,10-phenanthroline, Thermochim. Acta 466 (2007) 69–71, https://doi.org/10.1016/j.tca.2007.10.001.
[2] J.Z. Dàvalos, M.D-M.C. Ribeiro da Silva, M.A.V. Ribeiro Da Silva, V.L.S. Freitas, P. Jiménez, M.V. Roux, P. Cabildo, R.M. Claramunt, J. Elguero, Computational thermochemistry of six ureas, imidazolidin-2-one, N, N′-trimethyleneurea, benzimidazolinone, parabanic acid, barbital (5,5′-diethylbarbituric acid), and 3,4,4′-trichlorocarbanilide, with an extension to related compounds, J. Phys. Chem. A 114 (2010) 9237–9245, https://doi.org/10.1021/jp103514f.
[3] V.L.S. Freitas, J.R.B. Gomes, J.F. Liebman, M.D.M.C. Ribeiro da Silva, Energetic and reactivity properties of 9,10-dihydroacridine and diphenylamine: A comparative overview, J. Chem. Thermodyn. 115 (2017) 276–284, https://doi.org/10.1016/j.jct.2017.08.001.
[4] V.L.S. Freitas, M.D.M.C. Ribeiro da Silva, Thermochemical insights on small nitrogen heterocyclic compounds, in: A. Greer, J.F. Liebman (Eds.), The Chemistry of Nitrogen-Rich Functional Groups, PATAI's Chemistry of Functional Groups, John Wiley and Sons, July 2018, pp. 281–304, https://doi.org/10.1002/9780470682531.pat0933.
[5] A. Bencini, V. Lippolis, 1,10-Phenanthroline: A versatile building block for the construction of ligands for various purposes, Coord. Chem. Rev. 254 (2010) 2096–2180, https://doi.org/10.1016/j.ccr.2010.04.008.
[6] M. Mörtel, A. Witt, F.W. Heinemann, S. Bochmann, J. Bachmann, M. M. Khusniyarov, Inorg. Chem. 56 (2017) 13174–13186, https://doi.org/10.1021/acs.inorgchem.7b01952.
[7] A.I. Jothi, V. Alexander, Organic NLO material with H-bonded 1D helical self-assembly: synthesis, X-ray crystal structure, DFT calculations, SHG measurements and thermal studies of (5 Z, 6 E)-1, 10-phenanthroline-5, 6-dione dioxime, Cryst. Eng. Comm 19 (2017) 5251–5258, https://doi.org/10.1039/C7CE00743D.
[8] E. Shirakawa, K.-I. Itoh, T. Higashino, T. Hayashi, *Tert*-Butoxide-mediated arylation of benzene with aryl halides in the presence of a catalytic 1,10-phenanthroline derivative, J. Am. Chem. Soc. 132 (2010) 15537–15539, https://doi.org/10.1021/ja1080822.
[9] C. Bazzicalupi, A. Bencini, E. Berni, A. Bianchi, L. Borsari, C. Giorgi, B. Valtancoli, C. Lodeiro, J.C. Lima, A.J. Parola, F. Pina, Protonation and coordination properties towards Zn(II), Cd(II) and Hg(II) of a phenanthroline-containing macrocycle with an ethylamino pendant arm, Dalton Trans. 4 (2004) 591–597, https://doi.org/10.1039/B315608G.
[10] S. Fratini, M. Nikolka, A. Salleo, G. Schweicher, H. Sirringhaus, Charge transport in high-mobility conjugated polymers and molecular semiconductors, Nat. Mater. 19 (2020) 491–502, https://doi.org/10.1038/s41563-020-0647-2.
[11] T. Ji, Y.-K. Wang, L. Feng, G.-H. Li, W.-Y. Wang, Z.-F. Li, Y.-Y. Hao, Y.-X. Cui, Charge transporting materials for perovskite solar cells, Rare Metals 40 (2021) 2690–2711, https://doi.org/10.1016/bs.adioch.2018.05.009.
[12] M. Kim, J. Kim, H. Son, J.-H. Jang, M. Yi, Performance enhancement of organic thin-film transistors using bathophenanthroline: Cs electron injection layer, Jpn. J. Appl. Phys. 49 (2010) 101601, https://doi.org/10.1143/JJAP.49.101601.
[13] Y. Masumoto, T. Mori, Application of organic bathocuproine-based alloy film to organic light-emitting diodes, Thin Solid Films 516 (2008) 3350–3356, https://doi.org/10.1016/j.tsf.2007.11.082.
[14] H.R. Pouretedal, M.H. Keshavarz, Copper(I)-bathocuproine complex as carrier in iodide-selective electrode, Talanta 62 (2004) 221–225, https://doi.org/10.1016/S0039-9140(03)00398-9.
[15] C. Stenta, M.P. Montero-Rama, A. Viterisi, W. Cambarau, E. Palomares, L.F. Marsal, Solution processed bathocuproine for organic solar cells, IEEE Trans. Nanotechnol. 17 (2018) 128–132, https://doi.org/10.1109/TNANO.2017.2779544.
[16] T. Prohaska, J. Irrgeher, J. Benefield, J. Böhlke, L. Chesson, T. Coplen, T. Ding, P. Dunn, M. Gröning, N. Holden, H. Meijer, H. Moossen, A. Possolo, Y. Takahashi, J. Vogl, T. Walczyk, J. Wang, M. Wieser, S. Yoneda, X. Zhu, J. Meija Standard atomic weights of the elements 2021 (IUPAC Technical Report). *Pure Appl. Chem.* 94 (2022) 573-600. https://doi.org/10.1515/pac-2019-0603.
[17] NETZSCH-Gerätebau, Calibration set. DSC 214, 2022.
[18] G. Della Gatta, M.J. Richarson, S.M. Sarge, S. Stølen, Standards, calibration, and guidelines in microcalorimetry. Part 2. Calibration standards for differential scanning calorimetry* (IUPAC Technical Report), Pure Appl. Chem. 78 (2006) 1455–1476.
[19] R. Sabbah, A. Xu-wu, J.S. Chickos, M.L. Planas Leitão, M.V. Roux, L.A. Torres, Reference materials for calorimetry and differential thermal analysis, Thermochim. Acta 331 (1999) 93–204.
[20] F.A. Adedeji, D.L.S. Brown, J.A. Connor, W.L. Leung, I.M. Paz-Andrade, H. A. Skinner, Thermochemistry of arene chromium tricarbonyls and the strenghts of arene-chromium bonds, J. Organomet. Chem. 97 (1975) 221–228, https://doi.org/10.1016/S0022-328X(00)89468-1.
[21] L.M.N.B.F. Santos, B. Schröder, O.O.P. Fernandes, M.A.V. Ribeiro da Silva, Measurement of enthalpies of sublimation by drop method in a Calvet type calorimeter: design and test of a new system, Thermochim. Acta 415 (2004) 15–20, https://doi.org/10.1016/j.tca.2003.07.016.
[22] B. Brunetti, A. Ciccioli, G. Gigli, A. Lapi, N. Misceo, L. Tanzi, S. Vecchio Ciprioti, Vaporization of the prototypical ionic liquid BMImNTf(2) under equilibrium conditions: a multitechnique study, Phys. Chem. Chem. Phys. 16 (2014) 15653–15661, https://doi.org/10.1039/c4cp01673d.
[23] D.B. Newell, F. Cabiati, J. Fischer, K. Fujii, S.G. Karshenboim, H.S. Margolis, E. de Mirandes, P.J. Mohr, F. Nez, K. Pachucki, T.J. Quinn, B.N. Taylor, M. Wang, B. M. Wood, Z. Zhang, The CODATA 2017 values of h, e, k, and and NA for the revision of the SI, Metrologia 55 (2018) (2017) L13–L16, https://doi.org/10.1088/1681-7575/aa950a.
[24] A. Ciccioli, G. Gigli, The uncertain bond energy of the NaAu molecule: experimental redetermination and coupled cluster calculations, J. Phys. Chem. A 117 (2013) 4956–4962, https://doi.org/10.1021/jp402374t.
[25] J.S. Chickos, D.G. Hesse, J.F. Liebman, A group additivity approach for the estimation of heat capacities of organic liquids and solids at 298 K, Struct. Chem. 4 (4) (1993) 261–269, https://doi.org/10.1007/BF00673700.
[26] J.S. Chickos, S. Hosseini, D.G. Hesse, J.F. Liebman, Heat capacity corrections to a standard state: a comparison of new and some literature methods for organic liquids and solids, Struct. Chem. 4 (1993) 271–278, https://doi.org/10.1007/BF00673701.
[27] A. Arnau, Piezoelectric Transducers and Applications, Springer, 2004.
[28] C. Lu, A. Czanderna, Methods and Phenomena, Their Applications in Science and Technology. 1984.
[29] C. Steinem, A. Janshoff, Piezoelectric Sensors, Springer Science & Business Media, 2007.
[30] G. Sauerbrey, The use of quartz oscillators for weighing thin layers and for microweighing, Zeitschrift Für Physik 155 (1959) 206–222.

[31] V.M. Mecea, Fundamentals of mass measurements, J. Therm. Anal. Calorim. 86 (2006) 9–16, https://doi.org/10.1007/s10973-006-7570-x.
[32] S.P. Verevkin, R.V. Ralys, D.H. Zaitsau, V.N. Emel'yanenko, C. Schick, Express thermo-gravimetric method for the vaporization enthalpies appraisal for very low volatile molecular and ionic compounds, Thermochim. Acta 538 (2012) 55–62, https://doi.org/10.1016/j.tca.2012.03.018.
[33] S.P. Verevkin, D.H. Zaitsau, V.N. Emel'yanenko, A. Heintz, A new method for the determination of vaporization enthalpies of ionic liquids at low temperatures, J. Phys. Chem. B 115 (2011) 12889–12895, https://doi.org/10.1021/jp207397v.
[34] V.L.S. Freitas, P.J.O. Ferreira, M.D.M.C. Ribeiro da Silva, Experimental and computational thermochemical studies of acridone and N-methylacridone, J. Chem. Thermodyn. 118 (2018) 115–126, https://doi.org/10.1016/j.jct.2017.11.002.
[35] B. N. Taylor, C. E. Kuyatt, Guidelines for evaluating and expressing the uncertainty of NIST measurement results. NIST Technical Note 1297, 1994 Edition.